Science Advances
AAAS

advances.sciencemag.org/cgi/content/full/4/10/eaat5118/DC1

Supplementary Materials for

Organic synthesis on Mars by electrochemical reduction of CO_2

A. Steele*, L. G. Benning, R. Wirth, S. Siljeström, M. D. Fries, E. Hauri, P. G. Conrad, K. Rogers, J. Eigenbrode, A. Schreiber, A. Needham, J. H. Wang, F. M. McCubbin, D. Kilcoyne, Juan Diego Rodriguez Blanco

*Corresponding author. Email: asteele@carnegiescience.edu

Published 31 October 2018, *Sci. Adv.* **4**, eaat5118 (2018)
DOI: 10.1126/sciadv.aat5118

This PDF file includes:

Section S1. On the nature of contamination in these analyses

We conclude that the organic compounds analyzed in this study are indigenous to the meteorites studied and Mars for the following reasons;

- In thin sections, the thin section polymer and the problems associated with thin section analysis have been outlined elsewhere *(1)*, but it can be used as an indicator to show the path of possible contamination in the analyses. In Tissint, no thin section or polishing powders were associated with the inclusions analyzed and features shown in these analyses. In NWA 1950 and Nakhla, TEM, CRIS was able to distinguish between thin section polymer and in-situ organics based on its appearance, elemental signature or peak distribution respectively.

- Nakhla and Tissint are both falls and as such are minimally contaminated compared to finds such as NWA 1950. Tissint is the most pristine of the Martian meteorites and the inclusions analyzed where completely encased in the host maskelynite and reveal a similar peak and organic distribution to the other 2 meteorites. In Nakhla ~80% of the organic carbon in this meteorite has been shown to be Martian (*60*). In Tissint and NWA 1950 indigenous Martian phases have been reported (*1*).

- Samples for ToFSIMS were undertaken on fresh fracture surfaces free of any thin section polymers and were imaged by scanning electron microscopy after analysis to ensure no overt signs of contamination by terrestrial microbes was present in the analysis area (data not shown). in the case of Tissint, the high degree of correlation between ToFSIMS analysis of fresh fracture surfaces and STXM of sealed inclusions give a high degree of confidence in the nature of the organic carbon and its Martian provenance compared to the chemical signature of common laboratory contaminants or microbes (*60*).

- The δD from NanoSIMS analysis was conducted on the carbon rich phases found by CRIS to ensure that the analysis conducted was on Martian phases. Thin section polymer in these analyses had a δD of -150‰ while in NWA 1950 there was carbon rich phases corresponding to a δD of +98‰, in Nakhla +198 ‰ and in Tissint ~3000 ‰. These values are consistent with Martian magmatic signals in the case of Nakhla and NWA 1950 and with water that had equilibrated with the Martian atmosphere in the case of Tissint (see main text for references).

Section S2. The shock survival of indigenous martian organics

Although initially it may seem unlikely that the organics presented here would survive shock ejection from Mars, especially in NWA 1950 and Tissint which have experienced large shock events (between 35 - 45 GPa and a lower limit temperature delta of ~370^{o}C (*61*) for NWA 1950) and ~25 Gpa and 2000^{o}C for Tissint (*62*, *63*). However, in the case of NWA 1950 temperature sensitive chloromethane clathrate hydrates encased in MMC have been described that would degrade at <50^{o}C at terrestrial atmospheric pressure (Steele submitted alongside this paper). Both shock pressures and the temperature pulses during ejection are heterogeneous (as great as 1^{o}C per micron) and estimated to the bulk rock and may not have affected the MMC assemblages within inclusions, cracks and void spaces to a point where the P/T stability field of the material was exceeded (*64*). Indeed, Bland et al., (2014) reported simulations of shock effects in chondrites and have shown that temperature gradients of hundreds of degrees are expected within very small spatial scales (*65–68*). Therefore, the heterogeneity of shock and temperature processes favors the preservations of at least a small population of organic material. As to the effects of heat and shock on the nature of the organic material the observations of similar material on Mars by the SAM instrument (Eigenbrode et al., submitted) shows that at least a portion of the organic material on Mars survives impact ejection and transport to earth.

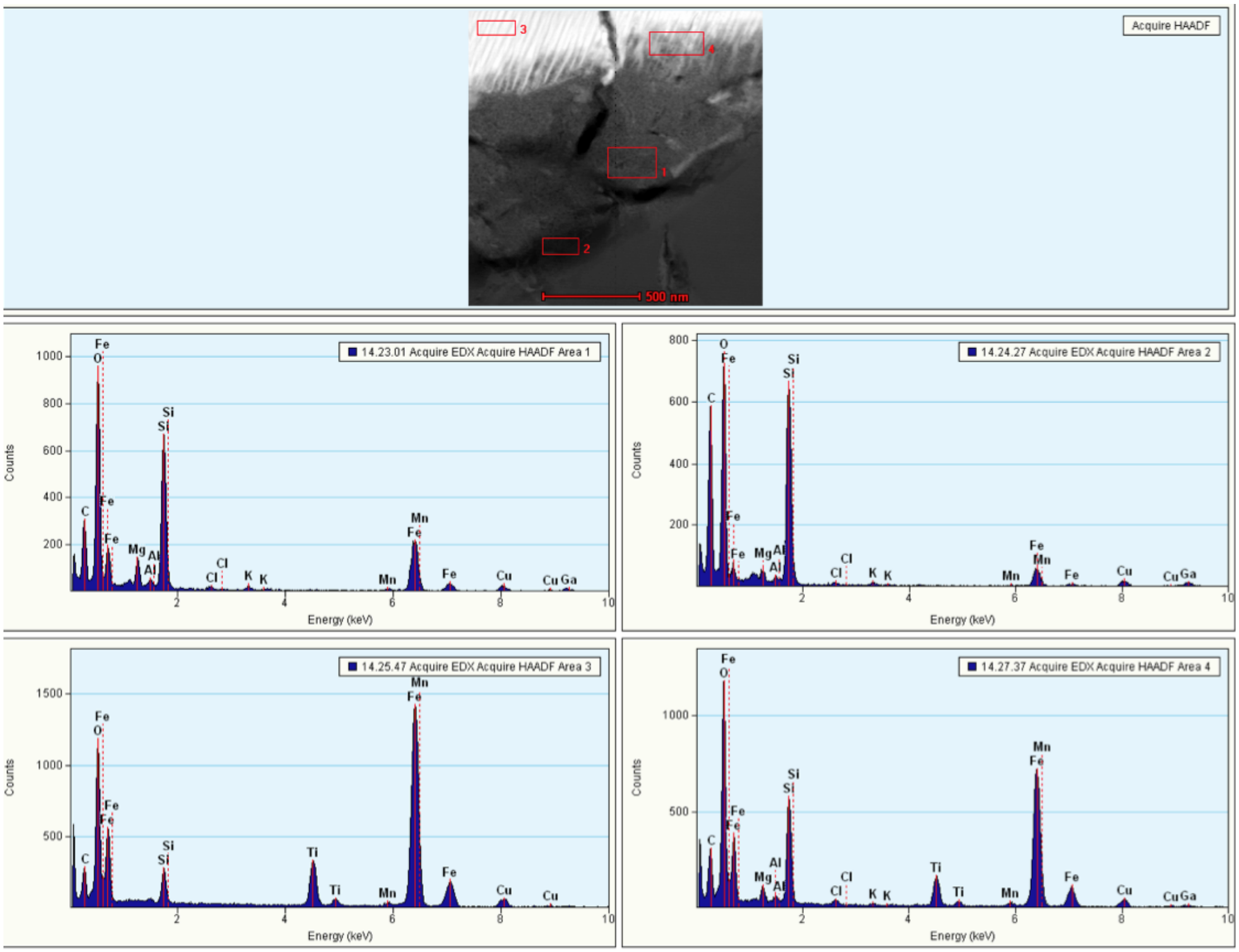

Fig. S1. Same titano-magnetite grain in Nakhla as imaged and shown in Fig. 2, illustrating the chemical composition of the sample from EDX spectra taken at several points.

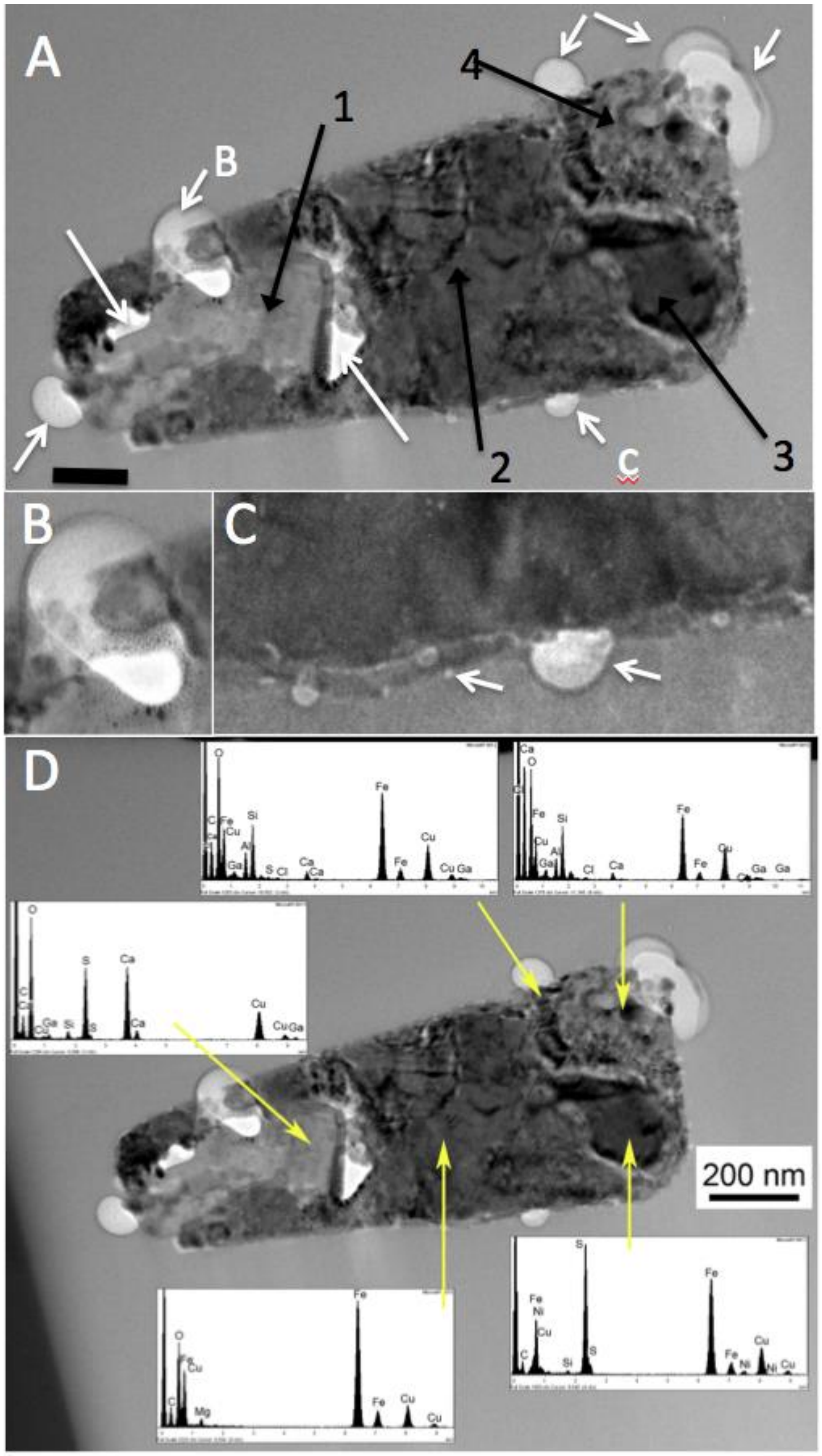

Fig. S2. Same inclusion in Tissint as imaged in TEM and shown in Fig. 4A, illustrating the chemical composition of the sample from EDX spectra taken at several points. See fig. S3 and table S1 for summary of electron diffraction analysis of the phases highlighted in this figure.

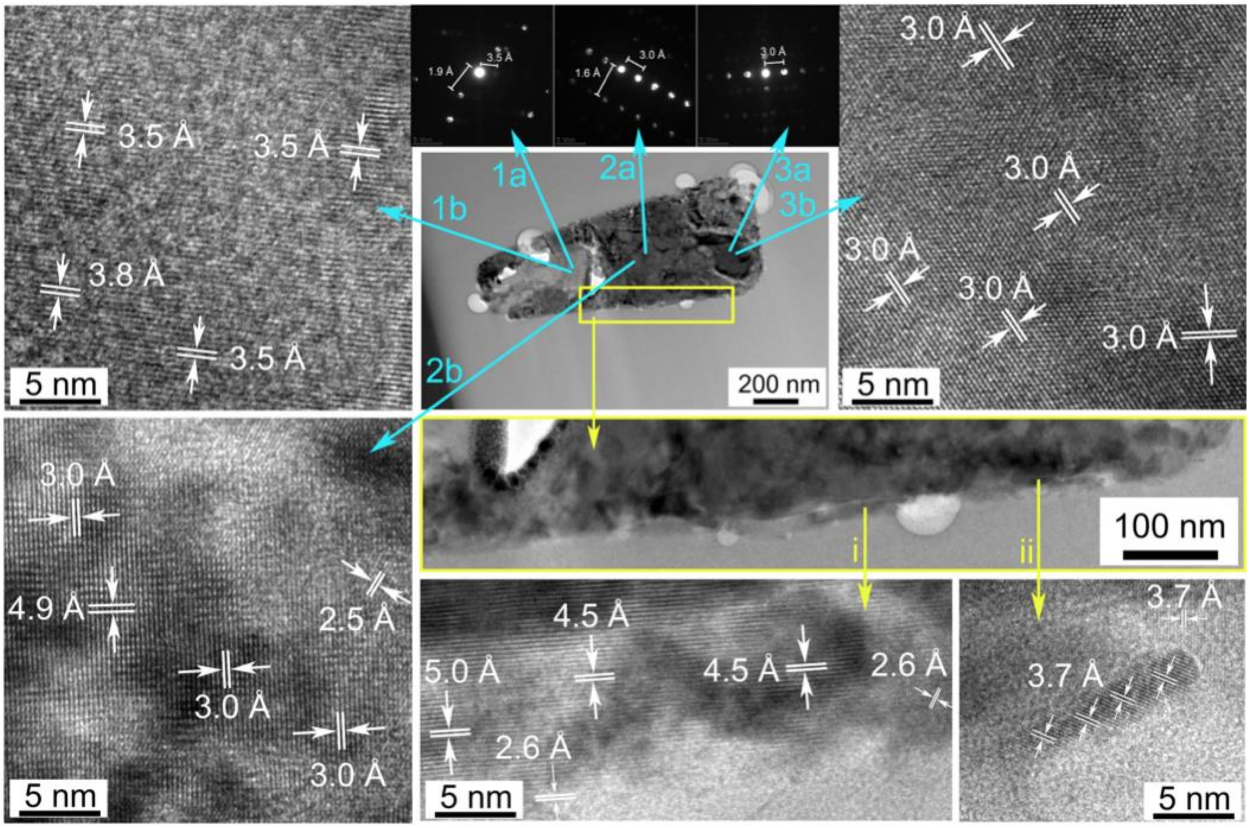

Fig. S3. Same inclusion as imaged in Fig. 4A and fig. S2 showing high-resolution TEM images of the measurements of lattice fringe dimensions and SAED patterns from each of the phases shown by blue arrows and reported in Fig. 4A.

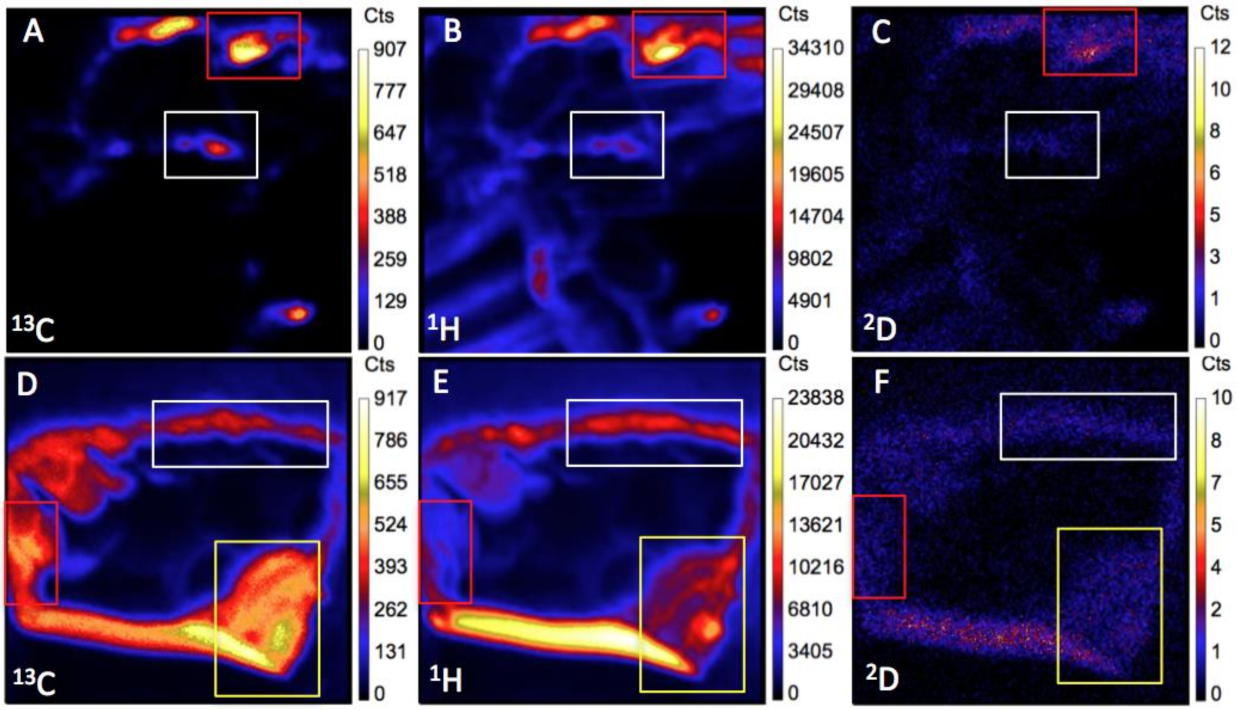

Fig. S4. NanoSIMS depth profile analysis of NWA 1950 (**A-C**) and Nakhla (**D-F**). In NWA 1950 the area corresponds to the titano-magnetite grain analyzed in Fig. 1A. (A) carbon 13 map, (B) hydrogen map, (C) deuterium map. In the boxed area shown in these images where H and D map to ^{13}C, the calculated δD ratios are: white box = -150 ± 43‰ and red box = 98 ± 20‰. Figures D – F are from the area of Nakhla shown in Fig. 1D and correspond to (D) carbon 13 map, (E) hydrogen map, (F) deuterium map. In the boxed area shown in these images where H and D map to ^{13}C, the calculated δD ratios are: white box = -25 ± 25‰, red box = 219 ± 60‰ and the yellow box = 32 ± 17‰.

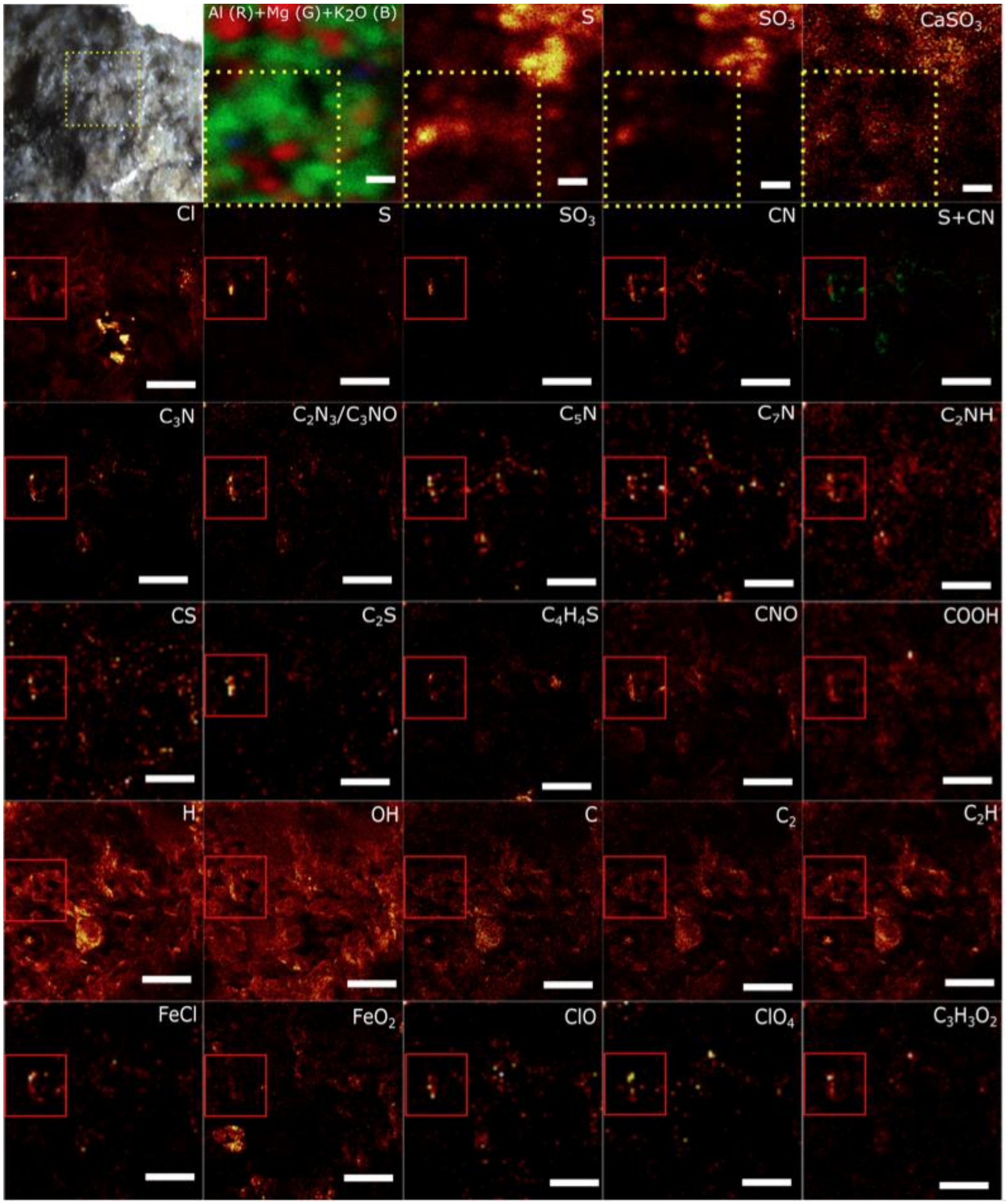

Fig. S5. Supplementary figure to complement Fig. 5 (ToF-SIMS analysis of Tissint); mass assignments are covered in table S2. The first image is a light microscope image of a fresh fracture surface of the Tissint meteorite as analyzed within the ToFSIMS instrument. The yellow box shows the area as analysed in the top row of ToFSIMS maps at low spatial resolution, individual species are identified on the image as a caption in the top right corner of the image and SOM Table 2. The yellow boxes in ion images in top row is the area for the set of higher spatial resolution images that make up the rest of the figure. Individual species are recorded in the top right of the individual images. The red boxes in the in ion images in second to sixth row denotes an area of concentration of many carbon, nitrogen, chlorine, iron and sulfur containing species that are labeled in the top right of the remaining images. The scale bars on the images are 20 μm.

.

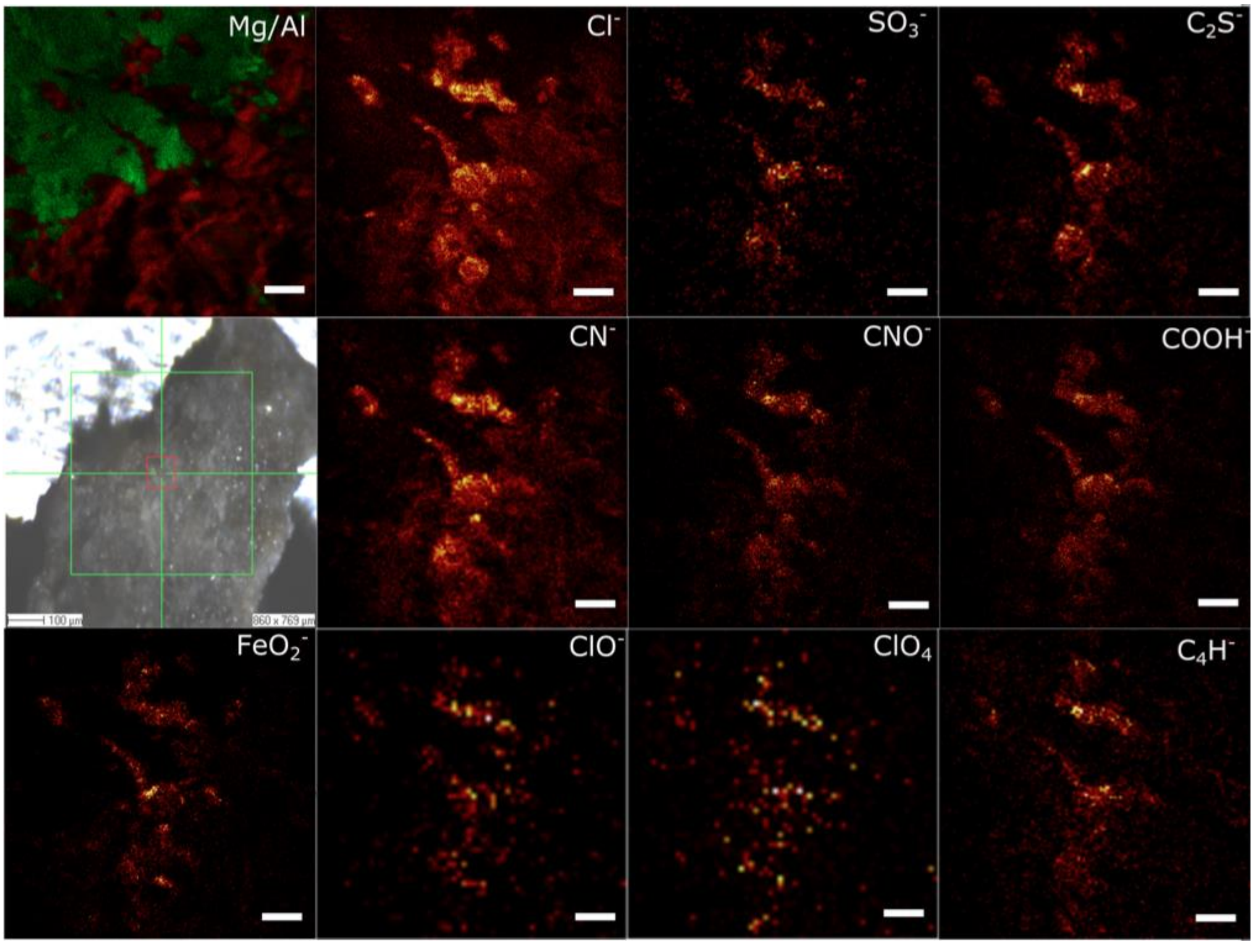

Fig. S6. ToF-SIMS analysis of a fresh fracture surface of Nakhla. Mass assignments are covered in table S3. Scale bars are 10 µm.

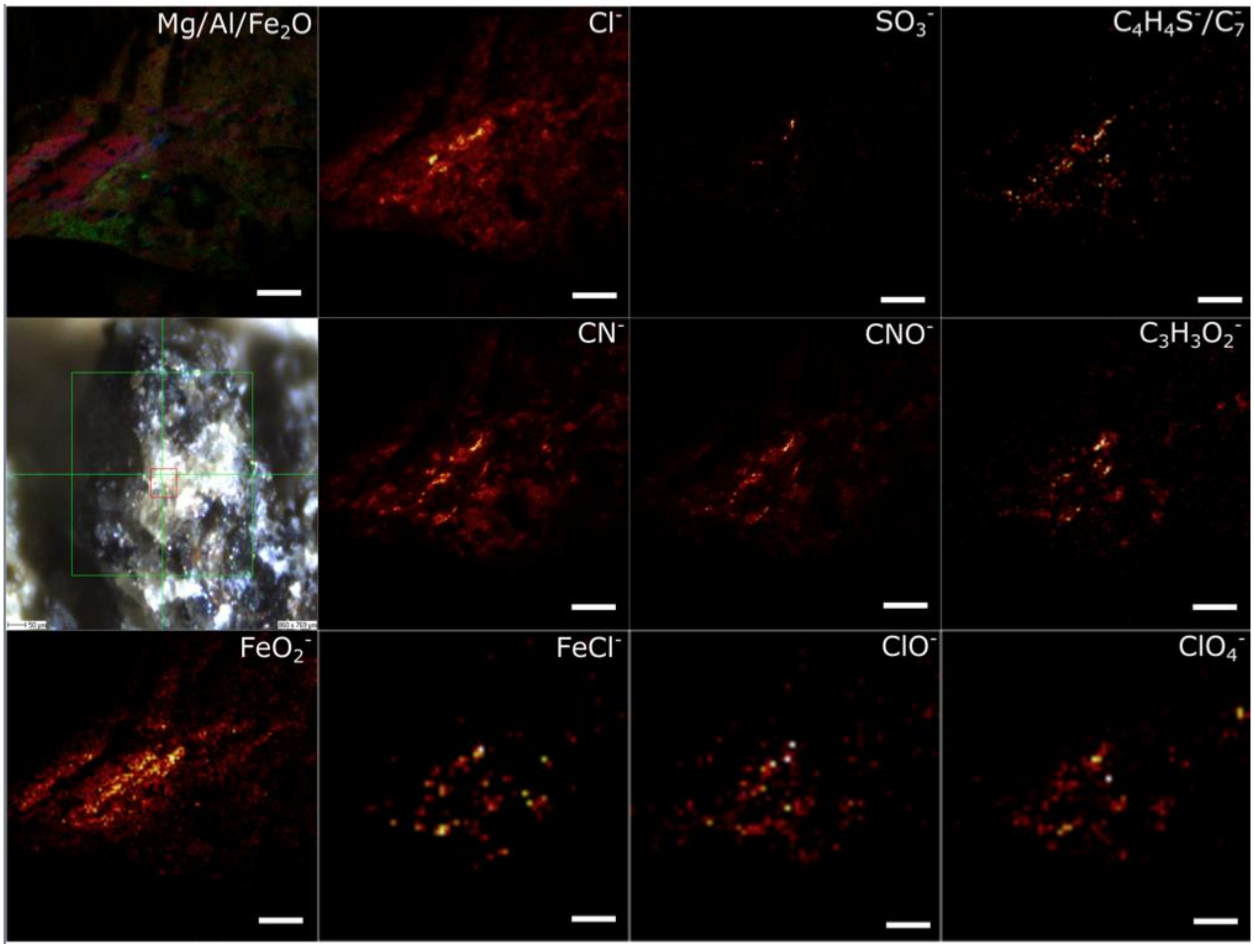

Fig. S7. ToF-SIMS analysis of a fresh fracture surface of NWA 1950. Mass assignments are covered in table S4 (see Steele et al., 2018 submitted). Scale bars are 10µm.

Table S1. Summary of d-space measurements on the areas marked in fig. S3 and the mineral identification from the ICDD database.

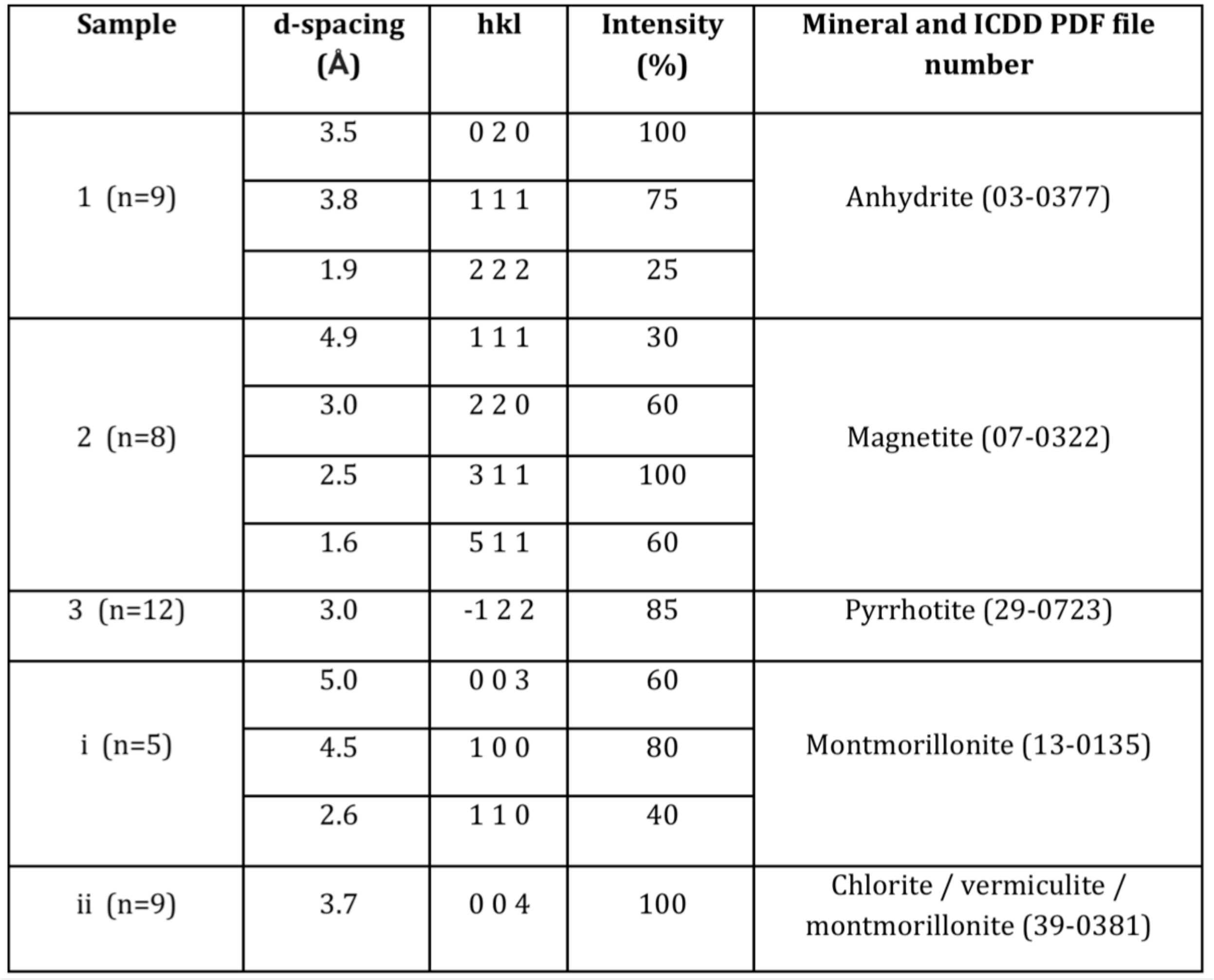

Sample	d-spacing (Å)	hkl	Intensity (%)	Mineral and ICDD PDF file number
1 (n=9)	3.5	0 2 0	100	Anhydrite (03-0377)
	3.8	1 1 1	75	
	1.9	2 2 2	25	
2 (n=8)	4.9	1 1 1	30	Magnetite (07-0322)
	3.0	2 2 0	60	
	2.5	3 1 1	100	
	1.6	5 1 1	60	
3 (n=12)	3.0	-1 2 2	85	Pyrrhotite (29-0723)
i (n=5)	5.0	0 0 3	60	Montmorillonite (13-0135)
	4.5	1 0 0	80	
	2.6	1 1 0	40	
ii (n=9)	3.7	0 0 4	100	Chlorite / vermiculite / montmorillonite (39-0381)

Table S2. This table pertains to Fig. 5 and fig. S5 and summarizes the mass peaks used to make the chemical designations (peak assignments) shown in these images. These pertain particularly to the high spatial resolution ion images of the ion species in row 2-6 (SOM Fig. 5). Due to the low mass resolution (m/Δm ~100–300) of this mode, peaks at the same nominal mass cannot be separated. Therefore, covering the same area, mass spectra of high mass resolution (m/Δm ~6000–8000) but low spatial resolution were also acquired. The ion images produced from these were compared with high spatial resolution to ensure that same spatial distribution. In most cases the interesting species were major species at the nominal mass.

Assignment	**Theoretical mass (*m/z*) of assignment**	**Observed mass (*m/z*) in high mass resolution mass spectrum**	**Comment to assignment**	**Other peaks at same nominal mass that might disturb high spatial resolution image**
C_2	24.00	24.00	No other likely assignments.	
C_2H	25.01	25.01	No other likely assignments.	
CN	26.00	26.00	No other likely assignments.	
CNO	42.00	42.00	No other likely assignments.	
COOH	44.998	44.998	CNF possible though unlikely as F has different spatial distribution.	Minor peak at *m/z* 44.98 (SiOH).
C_2NH	39.013	39.015	No other likely assignments.	Minor peaks at *m/z* 38.98 (NaO?) and 38.96 (K).
C_3N	50.00	50.01	NOFH possible though unlikely as F has different spatial distribution.	Minor peak at *m/z* 49.96 (^{34}SO) - SO_3 has different spatial distribution.
C_2N_3/C_3NO	66.01/66.00	66.000	C_2N_3 more likely considering spatial distribution of CNO.	Minor peak at *m/z* 65.95 ($^{34}SO_2$) – SO_3 has different spatial distribution.
$C_3H_3O_2$/ $C_2H_3N_2O$	71.013/71.024	71.019		Minor peak *m/z* 70.95 (KO_2?)
C_5N/C_2H_4SN	74.0036/74.0070	74.006	C_2H_4SN is less likely due to similarity of spatial distribution	Minor peak at *m/z* 73.94 ($^{57}FeOH$). FeO_2 has completely different spatial

			of C_5N and CN.	distribution.
C_7N/C_4H_4SN $C_3H_2N_2O_2$	98.0036/98.007/98.012	98.008	Maybe mixture of all species.	Major peak at *m/z* 97.94 (SO_4H) .SO_3 has different spatial distribution.
CS	43.97	43.97	SiO could contribute to this peak but it does not explain whole peak as Si and SiO_2 has very different spatial distribution compared to this peak.	Other minor peaks at *m/z* 44.01 (CH_2NO)
C_2S	55.97	55.97	SiCO could possibly contribute though does not explain whole peak as this peak has different spatial distribution than that of Si, C and SiC. It is likely CaO contribute a small part of the peak.	Minor peaks at *m/z* 55.93 (Fe) and 55.95 (Si_2). Fe and Si have different spatial distribution.
C_4H_4S/C_7	84.004/84.005	84.003	C_7 is unlikely when spatial distribution is compared with C_2, C_3 and C_4.	Minor peak at *m/z* 83.92 which is not found in area of interest but explain two other areas observed. Major peak at *m/z* 83.96 (ClO_3H?), 83.99 (?).
ClO	50.96	50.96	Could also be CK.	Major peak at *m/z* 51.02 (C_4H_3)
ClO_4	98.95	98.95		Minor peak at *m/z* 99.02 (C_8H_3)
FeO_2	87.92	87.93		Minor peak *m/z* 88.02 (C_3H_6SN?)
FeCl	90.90	90.92		Major peak at *m/z* 90.99 (?)

Table S3. This table pertains to ToF-SIMS analysis of Nakhla in fig. S6 and summarizes the mass peaks used to make the chemical designations (peak assignments) shown in these images. These pertain particularly to the high spatial resolution ion images fig. S6. Due to the low mass resolution (m/Δm ~100–300) of this mode, peaks at the same nominal mass cannot be separated. Therefore, covering the same area, mass spectra of high mass resolution (m/Δm ~6000–8000) but low spatial resolution were also acquired. The ion images produced from these were compared with high spatial resolution to ensure that same spatial distribution. In most cases the interesting species were major species at the nominal mass.

Assignment	**Theoretical mass (*m/z*) of assignment**	**Observed mass (*m/z*) in high mass resolution mass spectrum**	**Comment to assignment**	**Other peaks at same nominal mass that might disturb high spatial resolution image**
CN	26.00	26.00	No other likely assignments.	
CNO	42.00	42.00	No other likely assignments .	
COOH	44.998	44.998	CNF possible though unlikely as F has different spatial distribution.	Minor peak at *m/z* 44.98 (SiOH).
C_4H	49.01	49.01	No other likely assignments.	Minor peak at m/z 48.97 (SOH)
C_2S	55.97	55.97	SiCO could possibly contribute.	Minor peaks at m/z 55.93 (Fe) and 55.95 (Si_2).
ClO	50.96	50.96	Could also be CK though unlikely due different spatial distrubtion of K.	Minor peak at m/z 51.02 (C_4H_3)
ClO_4	98.95	98.95		
FeO_2	87.92	87.93		

Table S4. This table pertains to ToF-SIMS analysis of NWA 1950 in fig. S7 and summarizes the mass peaks used to make the chemical designations (peak assignments) shown in these images. These pertain particularly to the high spatial resolution ion images fig. S7. Due to the low mass resolution (m/Δm ~100–300) of this mode, peaks at the same nominal mass cannot be separated. Therefore, covering the same area, mass spectra of high mass resolution (m/Δm ~6000–8000) but low spatial resolution were also acquired. The ion images produced from these were compared with high spatial resolution to ensure that same spatial distribution. In most cases the interesting species were major species at the nominal mass.

Assignment	**Theoretical mass (*m/z*) of assignment**	**Observed mass (*m/z*) in high mass resolution mass spectrum**	**Comment to assignment**	**Other peaks at same nominal mass that might disturb high spatial resolution image**
CN	26.00	26.00	No other likely assignments	
CNO	42.00	42.00	No other likely assignments	
$C_3H_3O_2$/ $C_2H_3N_2O$	71.013/71.024	71.016	COOH show similar spatial distribution.	Peaks *m/z* 70.94 (MnO?) and 70.97.
C_4H_4S/C_7	84.004/84.005	84.001	Probably a mix of C_7 and C_4H_4S.	Major peak at *m/z* 83.95.
ClO	50.96	50.96	Could also be CK though unlikely due different spatial distribution of K.	Minor peak at *m/z* 51.02 (C_4H_3)
ClO_4	98.95	98.95		Minor peak at *m/z* 99.02 (?)
FeO_2	87.92	87.935		Minor peak *m/z* 88.02 (C_3H_6SN?)
FeCl	90.90	90.93		Major peak at m/z 90.99 (?)